frontiers | Frontiers in Earth Science

TYPE Original Research
PUBLISHED 09 January 2024
DOI 10.3389/feart.2023.1337998

OPEN ACCESS

EDITED BY
Roberto Alonso González-Lezcano,
CEU San Pablo University, Spain

REVIEWED BY
Yulong Cui,
Anhui University of Science and Technology, China
Eduardo López-Fernández,
CEU San Pablo University, Spain

*CORRESPONDENCE
Zhongkang Yang,
yangzhk@stu.scu.edu.cn

RECEIVED 14 November 2023
ACCEPTED 29 December 2023
PUBLISHED 09 January 2024

CITATION
Wei J, Wang D, Yang Z, Wang J, Li Y and Hu W (2024), Characteristics and mechanism of large deformation of a reservoir colluvial landslide-a case study of the Yulinerzu landslide in Xiluodu Reservoir, China.
Front. Earth Sci. 11:1337998.
doi: 10.3389/feart.2023.1337998

Characteristics and mechanism of large deformation of a reservoir colluvial landslide-a case study of the Yulinerzu landslide in Xiluodu Reservoir, China

Jinbing Wei[1], Dikai Wang[2], Zhongkang Yang[1,2]*, Jiexiong Wang[2], Yuming Li[2] and Wanyu Hu[2]

[1]College of Water Resource and Hydropower, Sichuan University, Chengdu, China, [2]Power China Chengdu Engineering Corporation Limited, Chengdu, China

The reactivation of colluvial landslides in reservoir banks poses a serious threat to the safety of hydropower projects and nearby towns. This study aims to research the morphological evolution of this type of landslides under the action of reservoir water and the impact of morphological evolution on landslide stability. The study focused on the Yulinerzu landslide, a large reactivated colluvial landslide in the Xiluodu Reservoir, China. Field surveys were conducted to analyze the geological structure of the landslide. *In situ* monitoring and surveys were used to obtain the deformation characteristics and morphological evolution of the landslide. A combined seepage-slope stability analysis was conducted to reveal the deformation mechanism. The results show that the reactivation of the Yulinerzu landslide is dominated by reservoir water fluctuations rather than rainfall. The underlying geological condition of the colluvial landslide is its hydrogeological structure, which causes the landslide to deform in a step-like manner during reservoir operation. With the accumulation of displacement and morphology evolution, the landslide displayed self-stabilizing characteristics. Therefore, in the stability analysis and risk assessment of large deformation landslides, it is essential to take into account not only the hydraulic effects of reservoir fluctuation but also the evolution of landslide morphology.

KEYWORDS

colluvial landslide, large deformation, morphological evolution, impoundingfilling-drawdown influence, combined seepage-slope stability modeling

1 Introduction

Colluvial landslides are landslides that occur within the Quaternary system or loose deposits predating the Quaternary period (He et al., 2008). These colluvial landslides are widely distributed in the mountain and ravine regions of southwest China, where numerous large hydropower stations have either been already built or are under construction. Here, the reactivation of colluvial landslides in the reservoir banks poses a serious threat to the safety of these hydropower projects and nearby towns (Chen et al., 2023; Deng et al., 2023).

The reactivation of reservoir landslides can be triggered by the combined or individual effects of reservoir water level variations and precipitation (Yin et al., 2016; Song et al., 2018;

Kafle et al., 2022). The reactivation of landslides within reservoirs can lead to different patterns of deformation and stability as a result of varying internal and external conditions. Some landslides may accelerate and fail, while others may slow down and reach a level of stability. For example, the Vajont landslide in Italy underwent sudden failure in 1963 after 3 years of creeping motions, accumulating a displacement of nearly 4 m before the catastrophe occurred (Alonso and Pinyol, 2010; Paronuzzi et al., 2013; Dykes and Bromhead, 2018). In contrast, the Central Landslide in northern Poland exhibited increased activity during three different periods after the initial filling of the Włocławek reservoir in the early 1970s. However, no movements have been recorded within the landslide since March 2011 (Kaczmarek et al., 2015). Understanding the motion patterns and dynamic processes of landslides after reactivation remains an area worthy of considerable attention.

The reactivation and evolution of reservoir landslides are influenced by three main types of factors: i) Hydraulic effects (Hu et al., 2015; Huang et al., 2016; Tang et al., 2019). Analyzing hydraulic effects often requires unsaturated hydro-mechanical coupled analysis as the seepage and deformation of a reservoir landslide are intimately coupled and, generally, cannot be analyzed independently of each other (Huang et al., 2018). ii) Variations of material properties. The physical and mechanical parameters of landslide materials may change due to the physical or chemical effects of water. After the reactivation of a reservoir landslide, its stability and dynamic process are mainly controlled by the residual strength of the slip zone. This residual strength is related to factors such as mineral composition, particle size distribution, rate effects, and thermal interactions (Wen et al., 2007; Pinyol et al., 2018; Alvarado et al., 2019). iii) Changes in geometry of landslides. The geological structure and geometry of landslides control their deformation patterns and mechanisms (Travelletti and Malet, 2012; Alonso et al., 2021). In addition to the geometric changes resulting from large deformations, reservoir landslides also experience significant changes due to bank collapse triggered by toe erosion (Huang and Gu, 2017; Tu and Deng, 2020).

The deformation of colluvial landslides tends to persist for an extended period and results in significant displacement. For active landslides, morphological evolution is a process-response function (Brunsden, 1999). Therefore, to reliably evaluate stability, a "dynamic" analysis is required instead of the traditional "static" approach (Du et al., 2013). However, the existing studies on the deformation mechanism of reservoir landslides are mainly based on the initial morphology of landslides and mainly focus on the study of hydromechanical effects and physical mechanics effects under the combined action of rainfall and reservoir water. Few studies have been conducted on the influence of landslide morphology evolution on landslide stability.

In this paper, we present a comprehensive analysis of the Yulinerzu landslide, a large reactivated colluvial landslide located in the Xiluodu Reservoir. Our study focused on the morphological evolution of the landslide under the action of reservoir water and its impact on the landslide's stability. Initially, field surveys were conducted to identify the main geometrical and geological characteristics of the landslide. The kinematic behavior and seasonal patterns were elucidated based on 8 years of GNSS deformation monitoring data, while the overall morphological evolution of the landslide was captured using a three-dimensional laser scanner and multi-beam underwater sonar. Finally, the deformation mechanism was analyzed through a combined seepage-slope stability analysis.

2 Geographical and geological settings

The Yulinerzu landslide is located on the right bank of the Xiluodu Reservoir, 39 km from Xiluodu Dam (Figure 1). The Xiluodu Hydropower Project is the world's fourth-largest hydropower project, located on the lower reaches of the Jinsha River in Southwest China, with a total installed capacity of 13,860 MW and a total reservoir capacity of up to 1.267×10^{10} m^3.

The Yulinerzu landslide is situated at the front edge of a mountain ridge (Figures 1C,D). The planform of the landslide is approximately rectangular (Figure 2A), with a width along the reservoir bank of about 450 m and a length of the vertical bank slope of nearly 700 m. The elevations of the rear and front edges are 780 m and 500 m, respectively (Figure 3). After the impounding of the reservoir, the front edge has been submerged beneath the water level. In its longitudinal direction, the landslide has a steep-gentle-steep structure. The upper and lower slopes range from 30° to 35°, whereas the middle segment is a gentle slope platform with a slope of 15° and a length of 200 m. The landslide has a maximum thickness of about 80 m and an estimated volume of about 8×10^6 m^3. The primary sliding direction aligns closely with the vertical river channel and is oriented at 235°.

The Yulinerzu landslide is a typical colluvial landslide. The main material of the accumulation is grayish-yellow or brownish-yellow gravel soil, with a gravel content of about 30% and particle sizes mostly ranging from 0.5 to 2.0 cm. The structure of the accumulation is relatively compact, and the surface of the downstream and front edge parts is covered by collapsed limestone blocks and gravel. The diameter of the blocks generally ranges from 0.1 to 0.5 m, with a maximum of 2 m.

The bedrock in the study area is primarily composed of Ordovician–Silurian sandstone, shale and argillaceous limestone. Bedrock outcrops within the landslide area are extremely rare due to the presence of slope residuals. The upstream boundary of the landslide is marked by a soil gully with a cutting depth of 3–5 m. On the upstream outer side of the landslide, medium-thick sandstone interbedded with thin shale is exposed along the highway scarp (Figure 2B), with an orientation of 140°–155° azimuth and beds dipping at an angle of 60°–70°. Additionally, on the right rear edge of the landslide, limestone bedrock is exposed due to movement of the sliding mass (Figure 2C). The occurrence of limestone is 142°∠56°, which is consistent with interbedding of sandstone and shale interbedding. Scratches and steps can be seen on the surface of the limestone stratum, indicating that it forms the sliding surface for the rear edge downstream boundary of the landslide. The slip band of the Yulinerzu landslide is mainly composed of yellow-brown silty clay with a small amount of gravel and has a thickness of 0.8–1.5 m (Figure 2D).

3 Deformation characteristics of the Yulinerzu landslide

3.1 Landslide activity features

Prior to the impoundment of Xiluodu Reservoir, the water level of Jinsha River was about 410 m. The Yulinerzu landslide was stable and did not show any signs of deformation.

The Yulinerzu landslide started to deform after the impoundment of the Xiluodu Reservoir, which began on 4 May

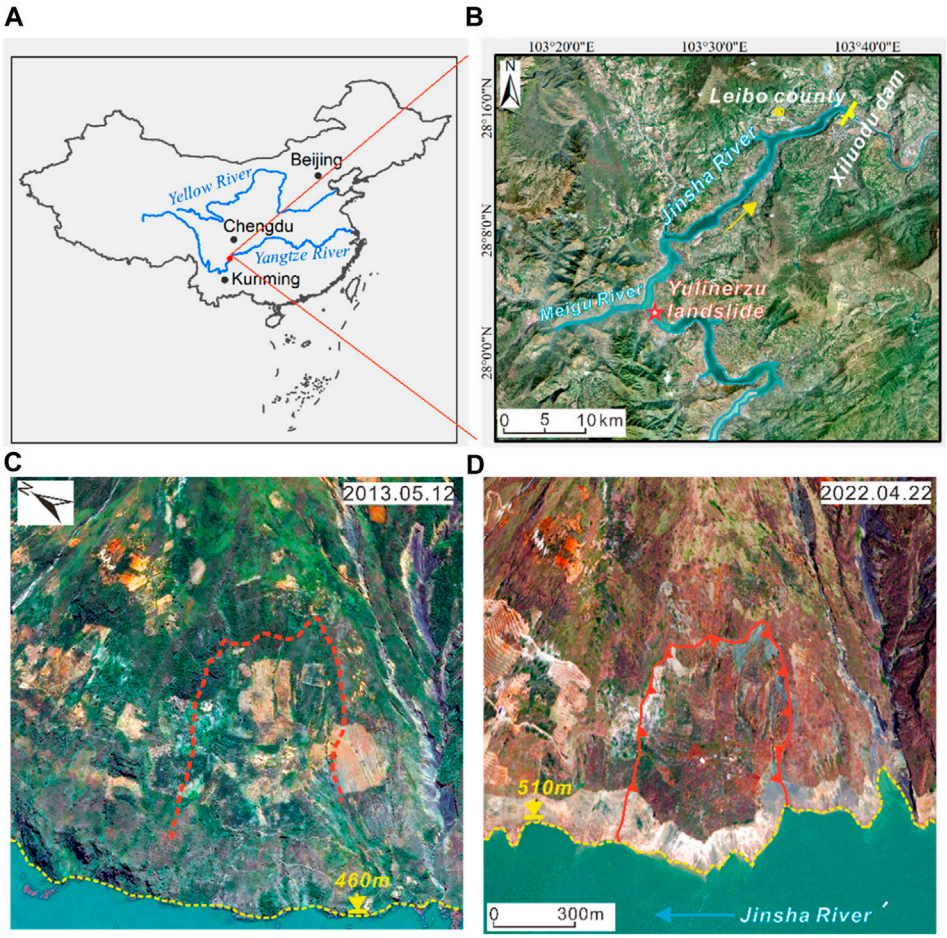

FIGURE 1
Location of the Yulinerzu landslide **(A,B)**. **(C)** Original overview when measurements started in 2013. **(D)** Overview in 2022.

2013. The reservoir level rose to an elevation of 500 m on June 6, corresponding to the front edge of the landslide. Field investigations of the Yulinerzu landslide revealed that deformation signs began to appear on June 19th, when the reservoir level reached 530 m. By June 26th, there were disturbance marks on the slope's gravel soil and numerous secondary cracks in both the rear and front edges. The width of the rear edge crack ranged between 30 and 60 cm, with a maximum of about 1.2 m and an estimated depth of over 5 m (Figure 4A). Disturbance marks on the slope's gravel soil were evident, and there were numerous secondary cracks in both the rear and front edges. The secondary cracks at the rear edge were generally 20–50 m long and 5–20 cm wide, with occasional steps of 5–10 cm in some areas. The secondary cracks at the front edge were relatively smaller, measuring 10–20 m in length and 0.5–3 cm in width (Figure 4B). Additionally, there were collapses along the reservoir bank.

On 31 July 2013, the reservoir level peaked at 554 m and then began to decline, dropping to 540 m by August 15th. During this drawdown period, the Yulinerzu landslide experienced intense deformation, with significant increases in crack width. The soil on both sides of the landslide collapsed and accumulated within the cracks, forming a stretching groove with a width of 5–8 m at the rear edge (Figure 4C). Secondary arc-shaped tensile cracks formed in the front parts of the slope, measuring from 3 to 5 cm up to about 10–20 cm in width. Some areas showed noticeable downward displacements, with a maximum of about 50 cm (Figure 4D). In addition, a bank collapse at the front edge of the slope increased the height by a maximum elevation of 25–30 m above the reservoir level.

On 29 September 2014, the reservoir water level reached its maximum designed elevation of 600 m and subsequently fluctuated between 600 m and 540 m. On-site investigations from 2014 to 2017 revealed that landslide deformation mainly occurred during periods of reservoir water level decline. After 2017, no further noticeable deformation of the landslide was observed. In December 2021, a combination of field investigation and unmanned aerial photography was used to determine the final distribution of cracks on the landslide, as shown in Figure 2A and Figure 5. The final height of the rear main scarp ranged between 8 and 26 m.

3.2 Deformation monitoring results

After the Yulinerzu landslide was found to be deforming, an automatic Global Navigation Satellite System (GNSS) consisting of nine displacement monitoring points was installed in September 2013 to monitor its surface displacement. The horizontal and

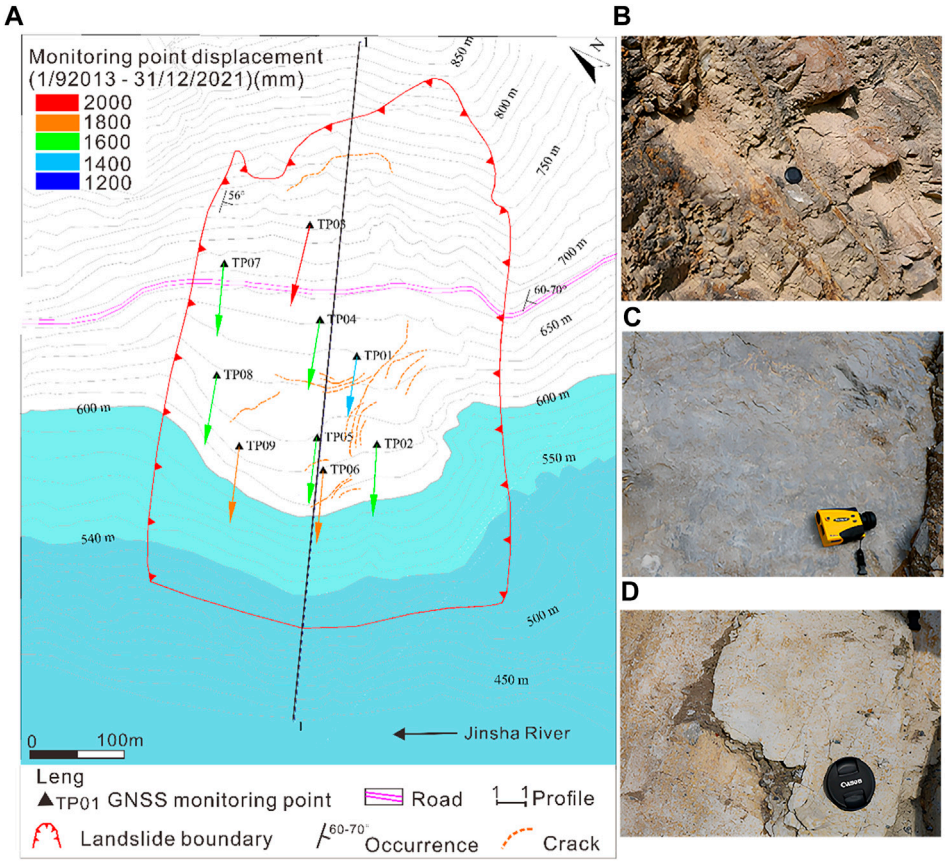

FIGURE 2
Planar map and outcrop characteristics of the Yulinerzu landslide. **(A)** Planar map and GNSS monitoring system, arrows show displacement magnitudes and directions from the GNSS points, **(B)** Outcrop on the upstream outer side, **(C)** Outcrop on the right rear edge, **(D)** Slip band on the rear edge.

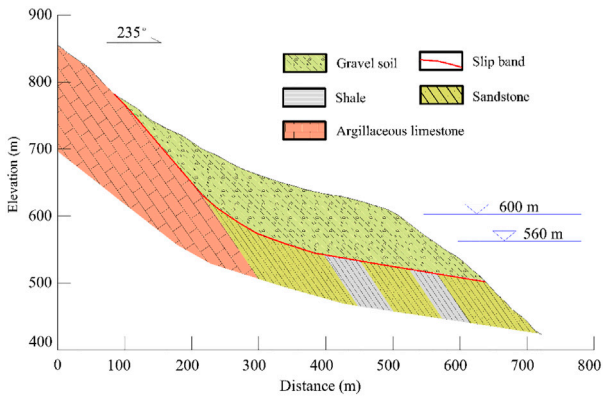

FIGURE 3
Original geology at cross section 1-1 (before reservoir impounding).

vertical accuracies of the GNSS displacement measurements were 5 mm and 10 mm, respectively. Concurrently, an automatic rain gauge was installed on the landslide to monitor precipitation, while reservoir level data were provided by the Xiluodu Hydropower Project's management.

The horizontal displacements of each GNSS monitoring point from September 2013 to December 2020 are shown in Figure 2A. Due to the submergence of the landslide's toe, the maximum displacement was recorded at the front of the middle gentle slope platform, followed by the upper part of the landslide. In contrast, the middle and rear parts of the gentle slope platform displayed the least displacement. Generally, the horizontal displacement of each point ranged from 11,281.4 mm to 14,701.3 mm, with a displacement orientation of 217°–242°. The similarity in the displacement magnitude and orientation at each point indicated that the landslide was characterized by overall movement.

The displacement-time curves of four GNSS points (TP03-06) at the main cross section 1-1 are shown in Figure 6, accompanied by the reservoir level and daily precipitation. These data show a close correlation between the movement of the landslide and the reservoir level fluctuation. However, there is no clear correlation with precipitation. The deformation of the landslide exhibits a stepwise growth trend over time. Apart from the initial storage year, when the rise in reservoir level triggered the reactivation of the landslide, subsequent movement mainly occurred during years of reservoir drawdown.

The deformation amplitude of the landslide decreased from 2014 to 2016, and then remained relatively stable after 2018 (Figure 7). In 2014, as the reservoir level dropped from 560 m to

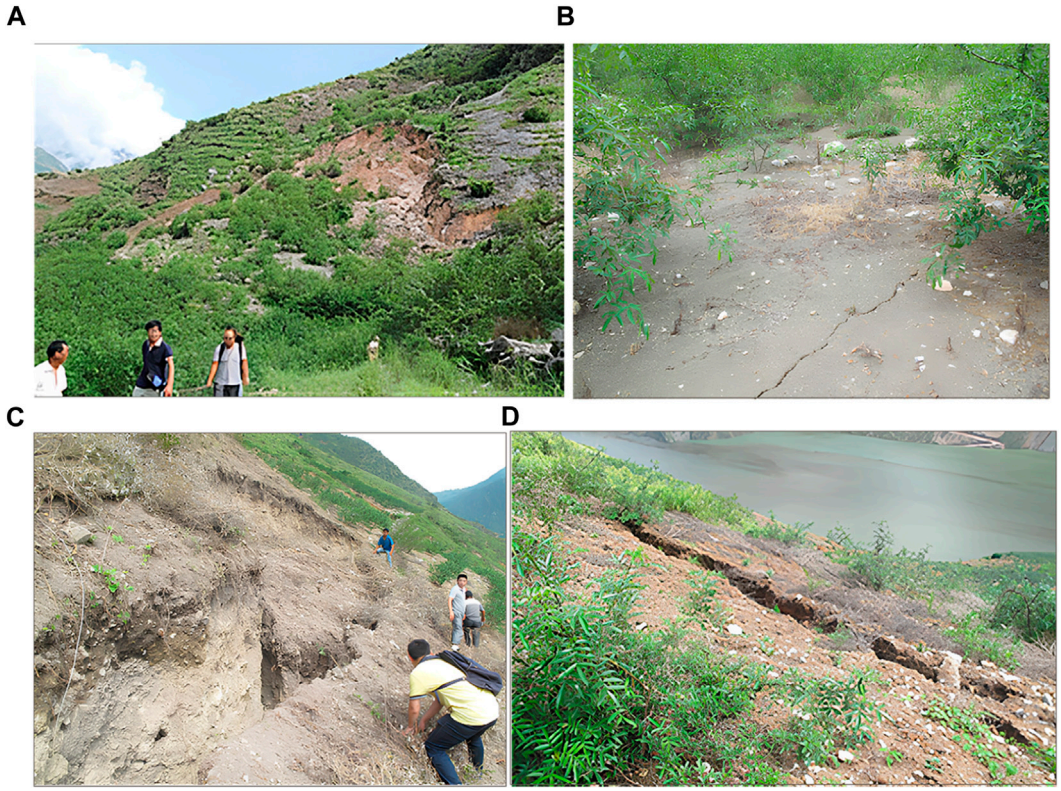

FIGURE 4
Cracks of the Yulinerzu landslide. **(A)** The initial crack at the rear edge, **(B)** The secondary cracks at the front edge, **(C)** Stretching groove at the rear edge, **(D)** Secondary arc-shaped tensile cracks in the front part.

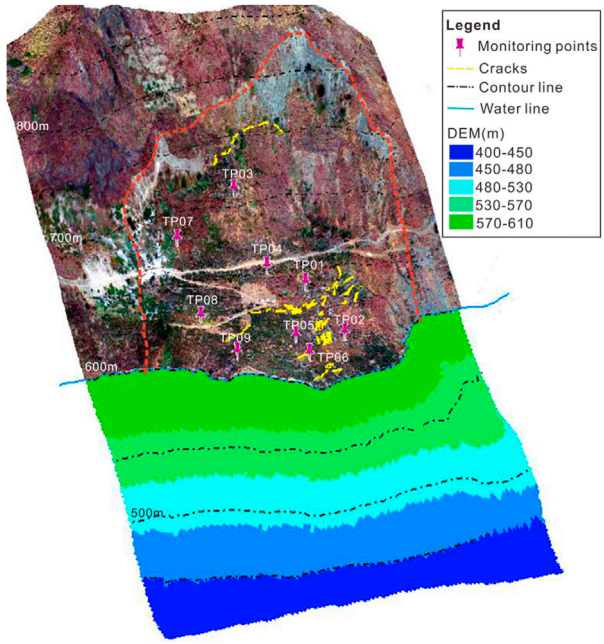

FIGURE 5
Final morphology of the Yulinerzu landslide.

540 m, the annual horizontal displacements of TP03-06 ranged between 3067.9 mm and 3740.5 mm. In 2015, the reservoir level experienced its first drop from its maximum operating elevation of 600 m to its minimum operating elevation of 540 m, resulting in annual displacements ranging from 4167.9 mm to 5102.1 mm, surpassing the previous year. In 2016, the reservoir level dropped for the second time from 600 m to 540 m, with annual displacements ranging from 1283.1 mm to 1468.8 mm, significantly lower than the previous year. After 2018, annual displacements further decreased to less than 100 mm.

Since the deformation patterns across the GNSS points are similar, the relationship between landslide movement velocity and reservoir level fluctuation was analyzed using TP05 as an example (Figure 8). Temporal variations in landslide velocities from 2014 to 2017 show a rapid activation during reservoir drawdown, reaching peak velocities (25–130 mm/day). In contrast, during rest periods, velocities decreased to their minimum. Additionally, the initiation of landslide movement slightly lags behind the rapid decline of the reservoir level. This phenomenon indicates that the movement of the landslide is mainly caused by the unfavorable hydraulic gradient within the slope resulting from the drop in reservoir water level. The peak value of landslide movement speed decreased annually until 2018, after which, even during periods of rapid reservoir level decline, it was no longer significant.

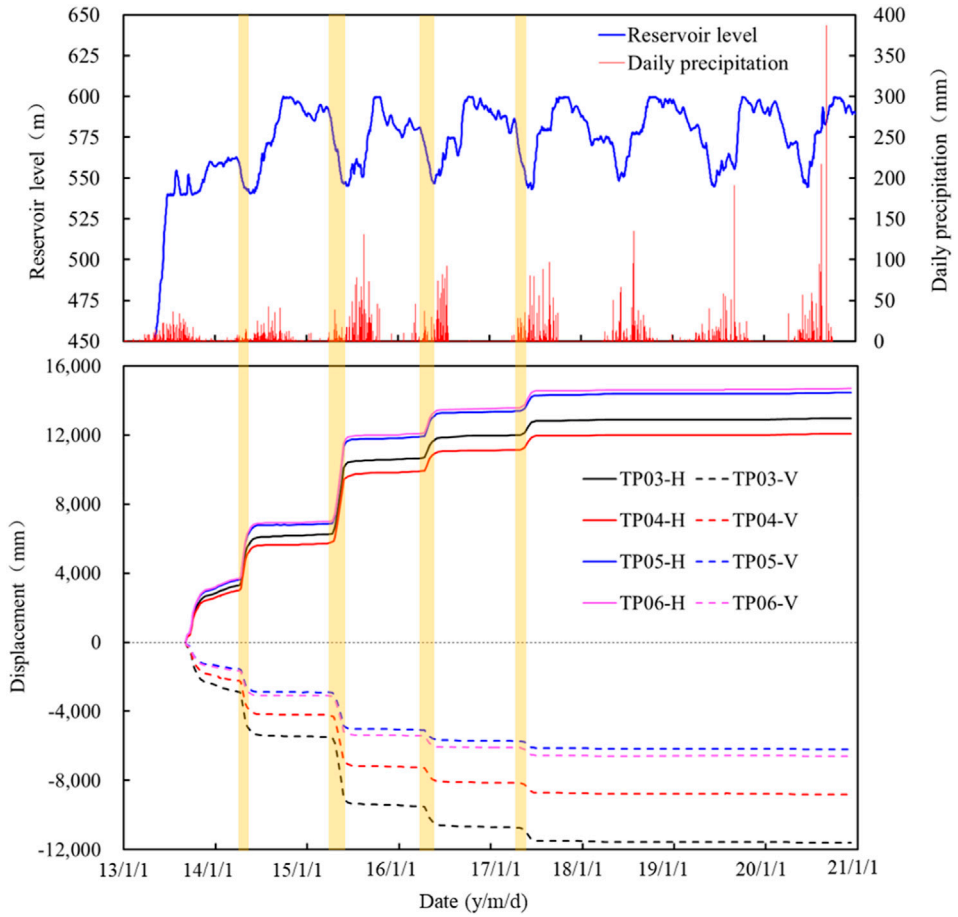

FIGURE 6
Temporal relationship between displacements of GNSS points in section 1-1 and associated reservoir level and precipitation.

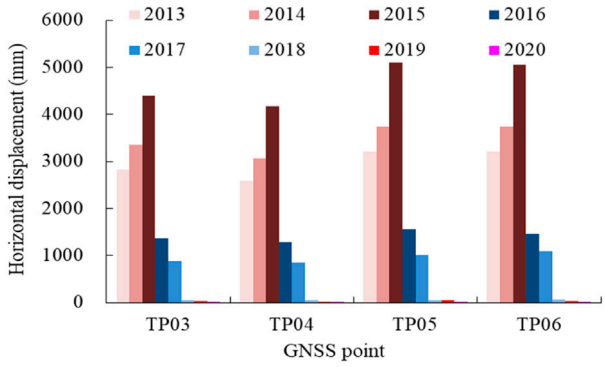

FIGURE 7
Annual horizontal displacements at GNSS points at section 1-1.

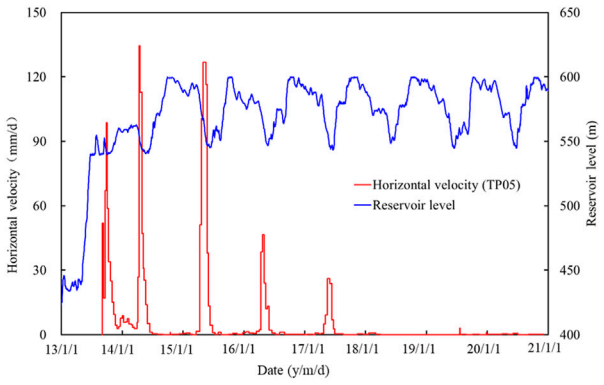

FIGURE 8
Comparison of horizontal velocities measured at TP05 and reservoir level fluctuation.

3.3 Morphological evolution of the sliding mass

As the landslide progressed towards the reservoir, its morphology changed due to differential displacements within the landslide and erosion at its front edge, ultimately affecting its overall stability. Significant displacements had already occurred from May to September 2013, predating the installation of the GNSS. Consequently, the GNSS did not capture the complete displacement of the landslide.

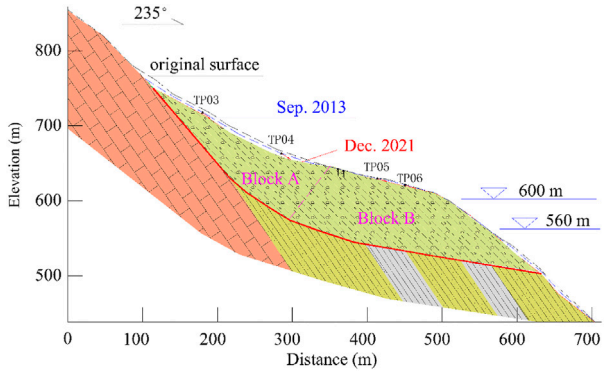

FIGURE 9
Morphological evolution of the landslide.

To comprehensively capture the morphological evolution, a multidimensional approach was employed in December 2021. A three-dimensional laser scanner was used to survey the surface morphology above the water level, while a combination of multi-beam underwater sonar and GNSS was used to survey the surface morphology below the water level. A GIS system was then used to integrate these datasets, resulting in a complete surface morphology (Figure 5). Comparing this dataset with the topographic map prior to reservoir impounding and combining it with the measured displacement vectors obtained through GNSS monitoring, the entire morphological evolution of the sliding mass was reconstructed (Figure 9).

The stability of a landslide can be influenced by toe erosion, a process characterized by bank sloughing, deformation, and retreat caused by the softening and erosion of the toe by reservoir water (Huang and Gu, 2017). However, the slope gradient of the Yulinerzu landslide front remained relatively unchanged during the reservoir operation period, as shown by the underwater topography survey results. The shear outlet of the Yulinerzu landslide, which was higher than the riverbed, led to the collapse in the section protruding from the original slope due to displacement. Consequently, the influence of toe erosion on this landslide's stability was minimal. Overall, as the landslide progressed towards the reservoir, the main change in its geometry was the reduction in volume and a corresponding drop in the center of gravity of the upper block. In contrast, the geometry change of the lower block was very small, contributing to the overall stability of the landslide.

4 Combined seepage–slope stability analyses

As highlighted above, the potential trigger of the Yulinerzu landslide movement was the fluctuation of the reservoir water level. The Xiluodu Reservoir is an annual regulating reservoir with similar fluctuations in water level from year to year. However, the deformation magnitude of the Yulinerzu landslide decreased with each passing year and the landslide gradually approached stability in the absence of new external loads. A combined seepage–slope stability modeling was performed to investigate the influence of the repeated impounding and drawdown cycles of the Xiluodu

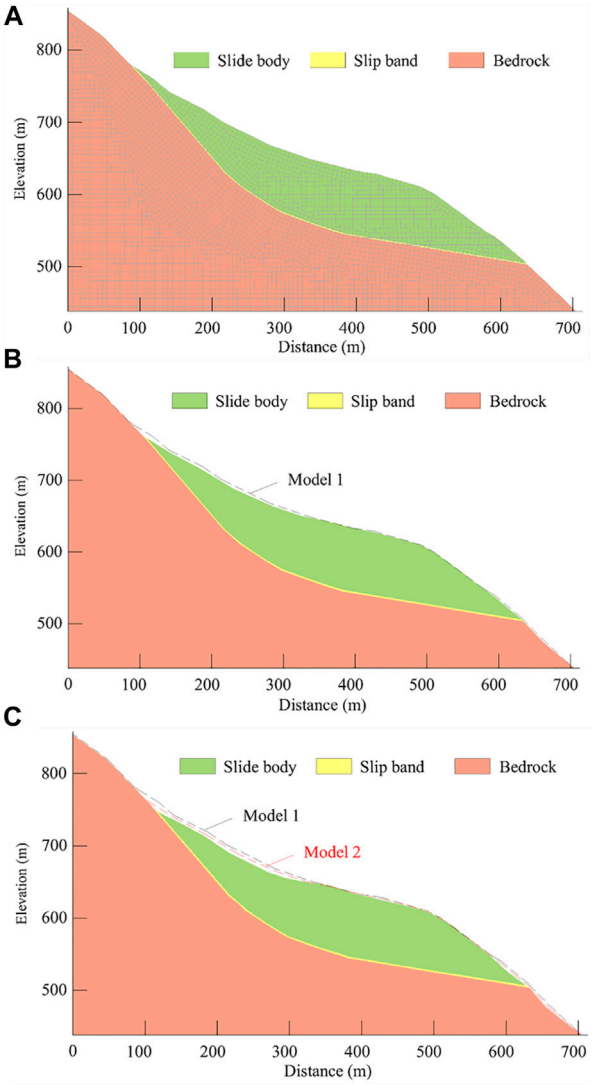

FIGURE 10
Calculation models of section 1 at different stages. **(A)** Model 1 (original morphology). **(B)** Model 2 (intermediate morphology). **(C)** Model 3 (final morphology).

Reservoir on the stability of the Yulinerzu landslide. Transient seepage simulation was implemented using the 2D finite element code of GeoStudio SEEP/W (Geo-Slope International Ltd, 2007). The results of the seepage simulation have subsequently been used for the slope stability analysis, employing the limit equilibrium code of SLOPE/W (Geo-Slope International Ltd, 2007) to evaluate the variations in the factor of safety (FOS) induced by reservoir impounding-drawdown cycles. The numerical study also focused on the morphological evolution of the landslide.

4.1 Model assumptions

The combined seepage-slope stability model of the Yulinerzu landslide is presented in Figure 10, delineated along cross section 1-1' (Figure 3). The model divides the cross-section into three hydrogeological-geomechanical units, namely, slide mass, slip

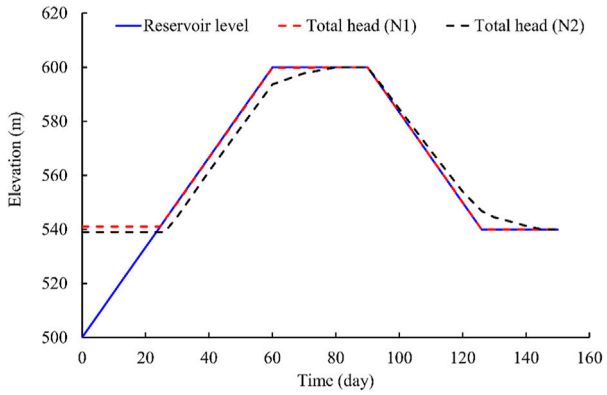

FIGURE 11
Variation of the total head above and below the slip band caused by reservoir level fluctuation (The positions of N1 and N2 are indicated in Figure 13A).

band and bedrock. Based on the morphological evolution of the landslide (Figure 9), three different geometries were considered: i) Model 1 corresponds to the original morphology before reservoir impoundment; ii) Model 2 represents the intermediate morphology during landslide movement corresponding to September 2013; iii) Model 3 corresponds to December 2021 and represents the landslide morphology after restoring stability.

The choice of initial and boundary conditions plays a crucial role in transient seepage modeling (Paronuzzi et al., 2013). Here, a horizontal water table level (500 m) was used as an initial condition in the seepage simulations. Variations in reservoir level during an impounding-drawdown cycle (Figure 11) were modeled through a hydraulic total head boundary condition assigned to the toe of the landslide. According to the actual operation of the reservoir, the rate of rise and fall of the reservoir water level was taken as 1.5 m/d. To reduce calculation time, the duration of the reservoir water lever at its highest and lowest points was shortened.

Transient seepage simulation requires the characterization of materials under unsaturated conditions (Pinyol et al., 2012). The Fredlund and Xing methods (Fredlund et al., 1994a, b) were used to develop the volumetric water content functions and hydraulic conductivity functions. The physical and hydrogeological properties adopted for the three hydrogeological units are indicated in Table 1 and the corresponding hydraulic functions are shown in Figure 12. The shear strength parameters were back-calculated based on the stability and observed failure process, with initial trial values determined from laboratory tests.

4.2 Results of unsaturated seepage calculation

The groundwater table variation caused by the reservoir level fluctuation is depicted in Figure 13. As the reservoir level changes, the groundwater table in the permeable sliding body is almost synchronized with the reservoir level. However, due to the low permeability of the slip band, the variation of groundwater level in the bedrock below the sliding zone lags behind that of the sliding body, creating a water head difference above and below the slip band (Figure 11). During the reservoir impounding period, the water head above the slip band is higher than below it, resulting in seepage pressure acting inward on the slope. This imparts some slope stability. Conversely, during the drawdown period, the water head above the slip band remains higher than that below it, leading to excess pore water pressure below the slip band. This condition is not conducive to slope stability.

4.3 FOS variations induced by impounding–drawdown cycles

Given the negligible impact of rainfall on the deformation of the Yulinerzu landslide, this paper only considered the influence of reservoir level changes on the stability of the landslide. The pore water pressure obtained from the seepage calculations was introduced into the limit equilibrium slope stability analyses using the Morgenstern-Price method and the SLOPE/W code (Geo-Slope International Ltd, 2007). The sliding surface, aligned with the slip band based on the geological interpretation, is governed by the widely used Mohr–Coulomb failure criterion, with strength parameters shown in Table 1.

The variations in stability conditions of the three different geometric models (Figure 12) throughout an entire impounding-drawdown cycle were calculated by combining seepage and slope stability analyses (Figure 14). The variation patterns of FOS with the reservoir level are similar for the three geometric models. The FOS decreases during the impoundment period and increases during the drawdown period. From the geometric shape, under the same reservoir level conditions, the FOS of Model 1 is the smallest and that of Model 3 is the largest.

Considering the dynamic evolution of geometric morphology, the slope stability trend reflected in the calculation is consistent with the actual situation of the Yulinerzu landslide during the impounding-drawdown cycle. Model 1 reflects the initial impoundment of the reservoir to an elevation of 554 m (until September 2014). When the water level rose to 530 m, the FOS of the landslide decreased to 0.997, and deformation of the landslide began to occur. Model 2 corresponds to the period from September 2014 to 2018. During this stage, except when the reservoir level decreased from 600 m to 570 m, the FOS of the landslide was less than 1. At other times, the FOS of the landslide was greater than 1. Therefore, the deformation of the landslide mainly occurred during the period of water level decline. Model 3 reflects the situation after 2018, when the FOS of the landslide was greater than 1, indicating that the landslide returned to a stable state.

5 Discussion

5.1 Hydraulics effect of the reservoir on landslide stability

The hydraulic effects of reservoir level changes on landslide stability can be divided into two aspects (Tang et al., 2019). The first is the floating effect. As the water level in the reservoir rises, the volume of the submerged slide mass increases, leading to an increase in water pressure on the sliding surface and a decrease in effective

TABLE 1 Material parameters of Yulinerzu landslide mass.

Parameters		Slide body	Slip band	Bedrock
Unit weight (kN/m^3)		22.5	22.7	24
Porosity		0.32	0.31	0.25
Saturated permeability/Ks (m/s)		5×10^{-4}	4×10^{-7}	5×10^{-6}
Frelund and Xing (1994), Frelund et al. (1994)	a (kPa)	5	10	8
	n	1.56	1.9	1.56
	m	0.5	0.22	0.4
Shear strength	Cohesion (kPa)	18	20	
	Friction angle (°)	26	21	

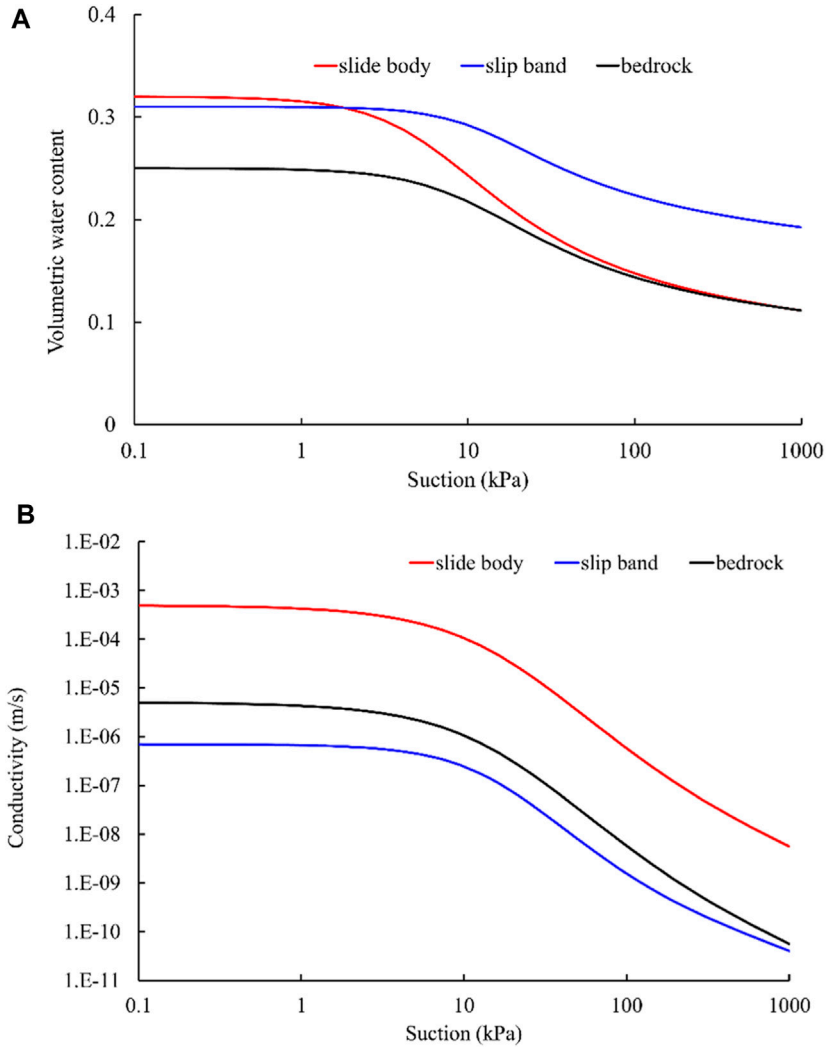

FIGURE 12
Hydraulic function adopted for the main hydrogeological units. **(A)** Soil-water characteristic curve. **(B)** Conductivity VS suction curve.

stress. Conversely, when the water level drops, the opposite occurs. The second effect is the seepage pressure effect, which generates a seepage pressure inward on the slope when the reservoir level rises and outward when it drops. These two effects have opposing impacts on landslide stability, and their relative magnitude determines the final impact on landslide stability.

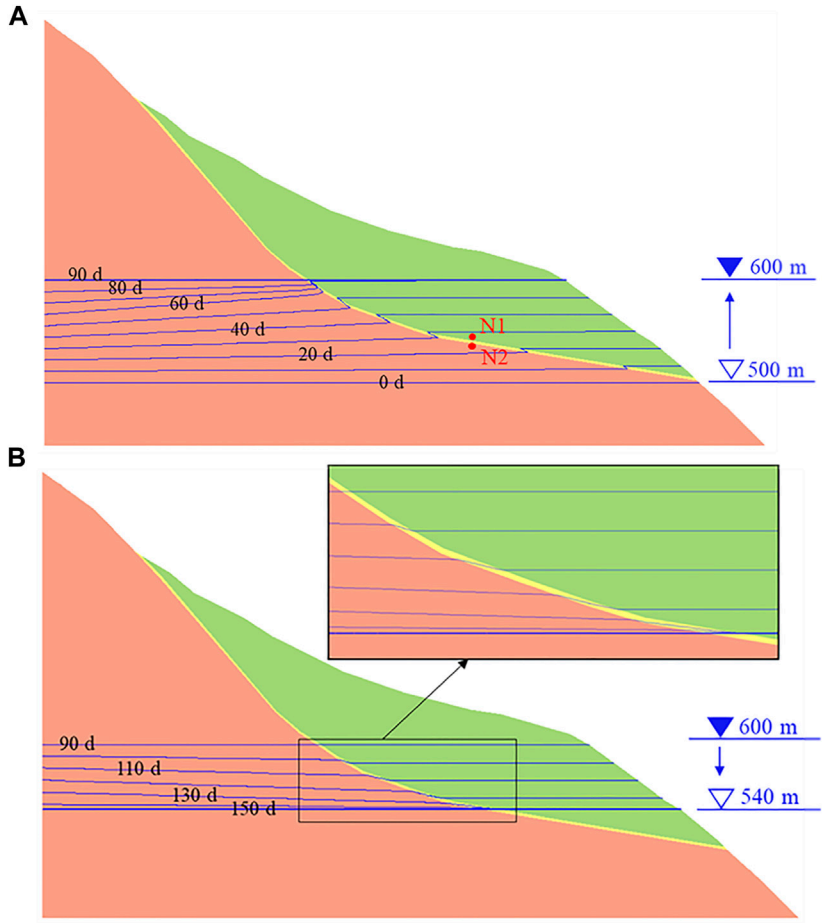

FIGURE 13
Groundwater table variations due to reservoir level fluctuations (Model 1). **(A)** Reservoir impounding. **(B)** Reservoir drawdown.

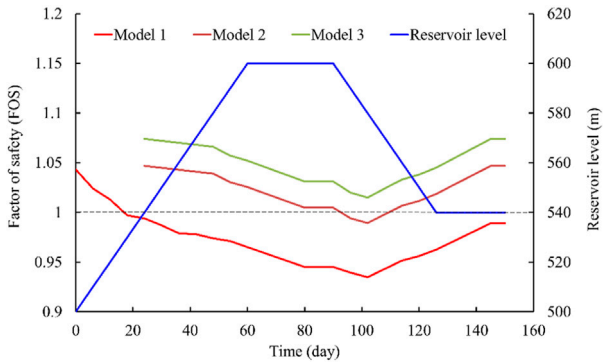

FIGURE 14
Factor of Safety (FOS) variations induced by impounding–drawdown cycles.

The floating effect and the seepage pressure effects are determined by the rate of reservoir level change, hydrogeological structure and hydraulic parameters of the landslide. Tang et al. (2019) analyzed and discussed the activity and displacements of reservoir landslides with special regard to different sliding surface and permeability and presented four dominant combinations of the inducing factors of reactive landslide. In their research, the hydrogeological structure of landslide was simplified as slide mass and bedrock. In the study of Canelles landslide, Pinyol et al. (2012) found that the hydraulic behavior of the clay layers where the sliding surface is located appears to be independent of the underlying sandstone. Due to the difficulty in dissipating or increasing water pressure within the clay, the failure of Canelles landslide is a result of rapid drawdown and the low water level reached in the reservoir. The Yulinerzu landslide is a colluvial landslide with a complex hydrogeological structure, characterized by a high permeability coefficient in the slide mass and a low permeability coefficient in the slip band, while the permeability coefficient of the bedrock below the slip band is relatively high. When the reservoir level changes, the groundwater level in the slide mass synchronizes with the reservoir level, and the seepage pressure is mainly manifested as the water head difference above and below the slip band. When the reservoir level rises, the adverse impact of the floating effect is greater than the beneficial impact of the seepage pressure effect, reducing the FOS of the landslide. Therefore, the floating effect is the main cause of deformation of the Yulinerzhu landslide during the initial impoundment. As the reservoir level continues to rise, the landslide regains its equilibrium due to its own morphological adjustment.

During the period of reservoir level decline, the adverse impact of the seepage pressure on landslide stability becomes greater than the beneficial impact of the floating effect, resulting in the lowest safety factor for the landslide and further deformation. This explains why the deformation of the Yulinerzu landslide lags behind the reservoir level decline. However, as the water level further decreases, the beneficial impact of the floating effect exceeds the adverse impact of seepage pressure, and thus the FOS of the landslide begins to increase, leading to a resumption of stability.

5.2 Influence of morphological evolution on landslide stability

The geometry of a landslide, especially the shape of its sliding surface, is an important factor affecting the deformation patterns, and failure behaviors, and their overall evolution. Sang et al. (2020) indicated that the strain distributions depend on the position of the main slip surface within the sliding zone, as well as the shear deformation of the sliding zone. Based on the difference in the dip angle of the sliding surface, the slide body of the Yulinerzu landslide was conceptually simplified into two blocks: an upper block with a sliding surface dip angle of 44°, and a lower block with a sliding surface dip angle of 12° (Figure 12). The upper block had a larger dip angle of the sliding surface, giving it a greater potential energy. When the resistance force of the lower block decreased under the action of the reservoir's water, the landslide manifested a tendency for revival deformation. Under the push of the upper block's high potential energy, the slide body moved forward as a whole, causing a proportional reduction in the upper block's potential energy. With the repeated rise and fall of the reservoir water level, the slide body was repeatedly activated and braked. This cycle weakened the potential energy of the upper block, gradually decreasing the overall deformation rate of the landslide decreased, until it stabilized.

Brunsden (2001) indicated that a landscape change takes place as a process–response function. Tang et al. (2015) investigated the evolutional characteristics of the Huangtupo landslide in the Three Gorges Reservoir region of China based on *in situ* tunneling and monitoring. Chen et al. (2023) analyzed the spatial distribution and failure mechanism of water-induced landslides in the reservoir areas of Southwest China. They found that as displacement accumulates, the movement of the landslide mass is a self-stabilizing process, however, they did not explain this mechanism. Based on the measured morphology evolution process of the Yulinerzu landslide, this paper used a limit equilibrium analysis method to analyze the safety factor of the landslide at different stages and obtained calculation results consistent with the actual situation.

Therefore, the morphological evolution caused by the accumulation of displacement is an important reason for the self-organizing characteristics of landslides. It is important to note that as the morphology of a landslide changes, its hydrogeological properties also change, which can affect its stability. This issue necessitates further research.

6 Conclusion

The paper provided a thorough investigation of the Yulinerzu landslide, which is a colluvial landslide located in the Xiluodu Reservoir. Based on the results of the study, we were able to draw the following conclusions:

(i) The impact of rainfall on the deformation of the Yulinezhu landslide was found to be negligible, while the fluctuation of the reservoir water level was the main factor that triggered its reactivation. The maximum deformation of the landslide occurred during the first impounding and drawdown period of the reservoir, showing a clear decelerating trend as the impounding–drawdown cycle progressed.

(ii) The hydrogeological structure of the colluvial landslide was the underlying geological factor that caused the landslide to deform in a step-like manner during reservoir operation. When the reservoir level increased, the floating effect became the primary factor contributing to landslide deformation, while when the reservoir level dropped, excess pore water pressure beneath the slip band emerged as the main factor causing landslide deformation.

(iii) The geometry of the landslide was found to be another important determinant of its deformation mode and evolution. The steep upper and gentle lower sliding surfaces of the Yulinerzu landslide made it prone to overall deformation. With the accumulation of displacement and morphological evolution, the landslide showed self-stabilizing characteristics. Therefore, in the stability analysis and risk assessment of large deformation landslides, it is essential to take into account not only the hydraulic effects of reservoir fluctuation but also the evolution of landslide morphology.

Data availability statement

The raw data supporting the conclusion of this article will be made available by the authors, without undue reservation.

Author contributions

JW: Writing–original draft, Writing–review and editing. DW: Data curation, Methodology, Resources, Writing–review and editing. ZY: Writing–original draft, Writing–review and editing. JW: Formal Analysis, Methodology, Resources, Software, Validation, Writing–review and editing. YL: Data curation, Supervision, Validation, Visualization, Writing–review and editing. WH: Investigation, Project administration, Supervision, Validation, Visualization, Writing–review and editing.

Funding

The author(s) declare financial support was received for the research, authorship, and/or publication of this article. This research was funded by the National Science Foundation of China (No. 41977246).

Conflict of interest

Authors DW, ZY, JW, YL, and WH were employed by Power China Chengdu Engineering Corporation Limited.

The remaining authors declare that the research was conducted in the absence of any commercial or financial relationships that could be construed as a potential conflict of interest.

Publisher's note

References

Alonso, E. E., and Pinyol, N. M. (2010). Criteria for rapid sliding I. A review of Vaiont case. *Eng. Geol.* 114, 198–210. doi:10.1016/j.enggeo.2010.04.018

Alonso, E. E., Sondon, M., and Alvarado, M. (2021). Landslides and hydraulic structures. *Eng. Geol.* 292, p106264. doi:10.1016/j.enggeo.2021.106264

Alvarado, M., Pinyol, N. M., and Alonso, E. E. (2019). Landslide motion assessment including rate effects and thermal interactions: revisiting the Canelles Landslide. *Can. Geotech. J.* 56 (9), 1338–1350. doi:10.1139/cgj-2018-0779

Brunsden, D. (1999). Some geomorphological considerations for the future development of landslide models. *Geomorphology* 30, 13–24. doi:10.1016/S0169-555X(99)00041-0

Brunsden, D. (2001). A critical assessment of the sensitivity concept in geomorphology. *Catena* 42, 99–123. doi:10.1016/S0341-8162(00)00134-X

Chen, M., Yang, X., and Zhou, J. (2023). Spatial distribution and failure mechanism of water-induced landslides in the reservoir areas of Southwest China. *J. Rock Mech. Geotech. Eng.* 15, 442–456. doi:10.1016/j.jrmge.2022.04.004

Deng, M., Huang, X., Yi, Q., Liu, Y., Yi, W., and Huang, H. (2023). Fifteen-year professional monitoring and deformation mechanism analysis of a large ancient landslide in the Three Gorges Reservoir Area, China. *B. Eng. Geol. Environ.* 82, p243. doi:10.1007/s10064-023-03262-9

Du, J., Yin, K., and Lacasse, S. (2013). Displacement prediction in colluvial landslides, three Gorges reservoir, China. *Landslides* 10, 203–218. doi:10.1007/s10346-012-0326-8

Dykes, A. P., and Bromhead, E. N. (2018). The Vaiont landslide: re-assessment of the evidence leads to rejection of the consensus. *Landslides* 15 (9), 1815–1832. doi:10.1007/s10346-018-0996-y

Frelund, D. G., and Xing, A. (1994). Equations for the soil-water characteristic curve. *Can. Geotech. J.* 31 (3), 521–532. doi:10.1139/t94-061

Frelund, D. G., Xing, A., and Huang, S. (1994). Predicting the permeability function for unsaturated soils using the soil-water characteristic curve. *Can. Geotech. J.* 31 (3), 533–546. doi:10.1139/t94-062

Geo-Slope International Ltd (2007). *Seepage and stability modeling with SEEP/W and SLOPE/W. Users Manuals*. Calgary, Alberta, Canada.

He, K., Li, X., Yan, X., and Guo, D. (2008). The landslides in the Three Gorges Reservoir region, China and the effects of water storage and rain on their stability. *Environ. Geol.* 55, 55–63. doi:10.1007/s00254-007-0964-7

Hu, X., Zhang, M., Sun, M., Huang, K., and Song, Y. (2015). Deformation characteristics and failure mode of the Zhujiadian landslide in the three Gorges reservoir, China. *B. Eng. Geol. Environ.* 74, 1–12. doi:10.1007/s10064-013-0552-x

Huang, D., and Gu, D. M. (2017). Influence of filling-drawdown cycles of the Three Gorges reservoir on deformation and failure behaviors of anaclinal rock slopes in the Wu Gorge. *Geomorphology* 295, 489–506. doi:10.1016/j.geomorph.2017.07.028

Huang, D., Gu, D. M., Song, Y. X., Cen, D. F., and Zeng, B. (2018). Towards a complete understanding of the triggering mechanism of a large reactivated landslide in the Three Gorges Reservoir. *Eng. Geol.* 238, 36–51. doi:10.1016/j.enggeo.2018.03.008

Huang, Q. X., Wang, J. L., and Xue, X. (2016). Interpreting the influence of rainfall and reservoir infilling on a landslide. *Landslides* 15 (10), 1139–1149. doi:10.1007/s10346-015-0644-8

Kaczmarek, H., Tyszkowski, S., and Banach, M. (2015). Landslide development at the shores of a dam reservoir (Włocławek, Poland), based on 40 years of research. *Environ. Earth. Sci.* 74, 4247–4259. doi:10.1007/s12665-015-4479-3

Kafle, L., Xu, W., Zeng, S., and Nagel, T. (2022). A numerical investigation of slope stability influenced by the combined effects of reservoir water level fluctuations and precipitation: a case study of the Bianjiazhai landslide in China. *Eng. Geol.* 297, p106508. doi:10.1016/j.enggeo.2021.106508

Paronuzzi, P., Rigo, E., and Bolla, A. (2013). Influence of filling-drawdown cycles of the Vajont reservoir on Mt. Toc slope stability. *Geomorphology* 191 (5), 75–93. doi:10.1016/j.geomorph.2013.03.004

Pinyol, N. M., Alonso, E., Corominas, J., and Moya, J. (2012). Canelles landslide: modelling rapid drawdown and fast potential sliding. *Landslides* 9, 33–51. doi:10.1007/s10346-011-0264-x

Pinyol, N. M., Alvarado, M., Alonso, E. E., and Zabala, F. (2018). Thermal effects in landslide mobility. *Géotechnique* 68 (6), 528–545. doi:10.1680/jgeot.17.P.054

Sang, H., Zhang, D., Gao, Y., Zhang, L., Wang, G., Shi, B., et al. (2020). Strain distribution based geometric models for characterizing the deformation of a sliding zone. *Eng. Geol.* 263, 105300–105310. doi:10.1016/j.enggeo.2019.105300

Song, K., Wang, F., Yi, Q., and Lu, S. (2018). Landslide deformation behavior influenced by water level fluctuations of the Three Gorges Reservoir (China). *Eng. Geol.* 247, 58–68. doi:10.1016/j.enggeo.2018.10.020

Tang, H., Li, C., Hu, X., Su, A., Wang, L., Wu, Y., et al. (2015). Evolution characteristics of the Huangtupo landslide based on *in situ* tunneling and monitoring. *Landslides* 12 (3), 511–521. doi:10.1007/s10346-014-0500-2

Tang, M., Xu, Q., Yang, H., Li, S., Iqbal, J., Fu, X., et al. (2019). Activity law and hydraulics mechanism of landslides with different sliding surface and permeability in the three Gorges Reservoir Area, China. *Eng. Geol.* 260, 105212. doi:10.1016/j.enggeo.2019.105212

Travelletti, J., and Malet, J. P. (2012). Characterization of the 3D geometry of flow-like landslides: a methodology based on the integration of heterogeneous multi-source data. *Eng. Geol.* 128, 30–48. doi:10.1016/j.enggeo.2011.05.003

Tu, G., and Deng, H. (2020). Formation and evolution of a successive landslide dam by the erosion of river: a case study of the gendakan landslide dam on the lancang river, China. *B. Eng. Geol. Environ.* 79, 2747–2761. doi:10.1007/s10064-020-01743-9

Wen, B. P., Aydin, A., Duzgoren-Aydin, N. S., Li, Y. R., Chen, H. Y., and Xiao, S. D. (2007). Residual strength of slip zones of large landslides in the Three Gorges area, China. *Eng. Geol.* 93, 82–98. doi:10.1016/j.enggeo.2007.05.006

Yin, Y., Huang, B., Wang, W., Wei, Y., Ma, X., Ma, F., et al. (2016). Reservoir-induced landslides and risk control in three Gorges project on Yangtze river, China. *J. Rock Mech. Geotech. Eng.* 8, 577–595. doi:10.1016/j.jrmge.2016.08.001